

Technical University of Denmark



## Anomalously high thermoelectric power factor in epitaxial ScN thin films

**Kerdsongpanya, Sit; Van Nong, Ngo; Pryds, Nini; Žukauskait, Agn; Jensen, Jens; Birch, Jens; Lu, Jun; Hultman, Lars; Wingqvist, Gunilla; Eklund, Per**

*Published in:*  
Applied Physics Letters

*Link to article, DOI:*  
[10.1063/1.3665945](https://doi.org/10.1063/1.3665945)

*Publication date:*  
2011

[Link back to DTU Orbit](#)

### *Citation (APA):*

Kerdsongpanya, S., Van Nong, N., Pryds, N., Žukauskait, A., Jensen, J., Birch, J., ... Eklund, P. (2011). Anomalously high thermoelectric power factor in epitaxial ScN thin films. *Applied Physics Letters*, 99, 232113. DOI: 10.1063/1.3665945

## DTU Library

Technical Information Center of Denmark

---

### General rights

Copyright and moral rights for the publications made accessible in the public portal are retained by the authors and/or other copyright owners and it is a condition of accessing publications that users recognise and abide by the legal requirements associated with these rights.

- Users may download and print one copy of any publication from the public portal for the purpose of private study or research.
- You may not further distribute the material or use it for any profit-making activity or commercial gain
- You may freely distribute the URL identifying the publication in the public portal

If you believe that this document breaches copyright please contact us providing details, and we will remove access to the work immediately and investigate your claim.

# Anomalously high thermoelectric power factor in epitaxial ScN thin films

Sit Kerdsonpanya<sup>\*a</sup>, Ngo Van Nong<sup>b</sup>, Nini Pryds<sup>b</sup>, Agnė Žukauskaitė<sup>a</sup>, Jens Jensen<sup>a</sup>, Jens Birch<sup>a</sup>, Jun Lu<sup>a</sup>, Lars Hultman,<sup>a</sup> Gunilla Wingqvist<sup>a</sup>, Per Eklund<sup>a</sup>

<sup>a</sup>Thin Film Physics Division, Department of Physics, Chemistry, and Biology (IFM), Linköping University, SE-581 83 Linköping, Sweden.

<sup>b</sup>Fuel Cells & Solid State Chemistry Division, Risø National Laboratory for Sustainable Energy, Technical University of Denmark, DK-4000 Roskilde, Denmark.

## ABSTRACT

Thermoelectric properties of ScN thin films grown by reactive magnetron sputtering on Al<sub>2</sub>O<sub>3</sub>(0001) wafers are reported. X-ray diffraction and elastic recoil detection analyses show that the composition of the films is close to stoichiometry with trace amounts (~1 at.% in total) of C, O, and F. We found that the ScN thin-film exhibits a rather low electrical resistivity of ~2.94 μΩ·m, while its Seebeck coefficient is approximately -86 μV/K at 800 K, yielding a power factor of ~2.5 × 10<sup>-3</sup> W/m·K<sup>2</sup>. This value is anomalously high for common transition-metal nitrides.

Keywords: Transition-metal nitride, Seebeck coefficient, X-ray diffraction, Electron microscopy

\* Corresponding author. E-mail [sitke@ifm.liu.se](mailto:sitke@ifm.liu.se)

26 Thermoelectric generators using thermoelectric materials directly convert heat into electricity  
27 by generating a potential difference in response to a temperature gradient (or vice versa). The  
28 conversion efficiency of a thermoelectric device depends on the thermoelectric figure of merit  
29 (ZT) at a certain temperature (T), where  $Z = S^2/(\rho \cdot \kappa)$  and S,  $\rho$ , and  $\kappa$  are the Seebeck  
30 coefficient, the electrical resistivity, and the thermal conductivity, respectively. Since S,  $\rho$ ,  
31 and  $\kappa$  are interdependent, it is a challenging task to improve ZT.<sup>1,2</sup> For typical thermoelectric  
32 materials,  $\kappa$  is dominated by the lattice thermal conductivity; the maximum ZT is then close  
33 the maximum of the parameter  $S^2/\rho$ , called the power factor. Here, we report a thermoelectric  
34 power factor of  $2.5 \times 10^{-3} \text{ W}/(\text{m} \cdot \text{K}^2)$  at 800 K for epitaxial ScN thin films due to a relatively  
35 high Seebeck coefficient of  $\sim 86 \mu\text{V}/\text{K}$  with low electrical resistivity ( $\sim 2.94 \mu\Omega \cdot \text{m}$ ). This is  
36 an anomalously high power factor for transition-metal nitrides and may place ScN-based  
37 materials as promising candidates for high temperature thermoelectric applications.

38  
39 Transition-metal nitrides have not been commonly considered for thermoelectric applications.  
40 Yet, they are much appreciated as wear-resistant coatings and electronic contacts materials  
41 because of their thermal and mechanical stability, electrical conductivity, and chemical  
42 inertness. Like many other transition-metal nitrides, ScN has high hardness and high melting  
43 point  $\sim 2900 \text{ K}$ .<sup>3,4</sup> It possesses a NaCl (B1) crystal structure with a lattice parameter of 4.521  
44 Å. For electrical properties, theoretical studies reported that ScN is an indirect semiconductor  
45 with energy gap in the range of 0.9-1.6 eV.<sup>5-9</sup> Measurements on as-deposited ScN show n-  
46 type behavior<sup>10,11</sup> and the carrier concentration of ScN has been reported to vary from  $10^{18}$  to  
47  $10^{22} \text{ cm}^{-3}$  with electron mobility of  $100\text{-}180 \text{ cm}^2\text{V}^{-1}\text{s}^{-1}$ .<sup>9,12-14</sup> These numbers of the carrier  
48 concentrations span the typical ideal range for thermoelectrics<sup>1</sup> while retaining a high carrier  
49 mobility;<sup>13</sup> a fact relevant to their thermoelectric power factor reported here.

50 ScN films were grown onto Al<sub>2</sub>O<sub>3</sub>(0001) substrates using reactive magnetron sputtering in an  
51 ultrahigh vacuum chamber with a base pressure of  $\sim 10^{-7}$  Pa. The chamber is described  
52 elsewhere.<sup>15</sup> The Sc target (99.99% purity specified as the amount of Sc divided by the total  
53 rare-earth metals in the target) has a diameter of 5 cm. The substrates were one-side polished  
54 Al<sub>2</sub>O<sub>3</sub>(0001) wafers. Prior to deposition, the substrates were degreased in an ultrasonic bath  
55 with trichloroethylene, acetone, and isopropanol for 5 min. each, and subsequently blown dry  
56 with N<sub>2</sub>. Before deposition, the substrates were heated in vacuum to the deposition  
57 temperature 800 °C (for 1 h for temperature stabilization and degassing). The Sc target was  
58 operated in dc mode (power-regulated) at a power of 80 W. The substrate was rotated during  
59 deposition in order to obtain uniform films. The depositions were performed in Ar/N<sub>2</sub> (flow  
60 ratio 87% Ar / 13% N<sub>2</sub>) with the total gas pressure at 0.2 Pa. Structural characterization of as-  
61 deposited films was performed by X-ray diffraction (XRD) using CuK<sub>α</sub> radiation.  $\theta$ -2 $\theta$  scans  
62 were measured in a Philips PW 1820 diffractometer;  $\phi$ -scans and pole figures were measured  
63 in a Philips X'pert Materials Research Diffractometer operated with point focus, primary  
64 optics of 2 × 2 mm cross slits, and secondary optics with parallel-plate collimator. The  $\phi$ -scan  
65 of ScN 200 peak was scanned with a fixed 2 $\theta$  angle of 40.16°, a fixed tilt angle ( $\psi$ ) of 54.7°,  
66 and azimuth-angle ( $\phi$ ) range 0-360° with step size 0.1°. Cross-sectional specimens for  
67 transmission electron microscopy (TEM) were prepared by gluing two pieces of the sample  
68 face to face and clamped with a Ti grid, polishing down to 50  $\mu$ m thickness. Ion milling was  
69 performed in a Gatan Precision Ion Polishing System (PIPS) at Ar<sup>+</sup> energy of 5 kV and a gun  
70 angle of 5°, with a final polishing step with 2 kV Ar<sup>+</sup> energy and angle of 2°. TEM  
71 characterization was performed using a Tecnai G2 TF20UT with a field-emission gun (FEG).  
72 Compositional analysis of as-deposited film was performed by time-of-flight elastic recoil  
73 detection analysis (ToF-ERDA). Here, a 30 MeV <sup>127</sup>I<sup>9+</sup> beam was directed to the films at an  
74 incident angle of 67.5° with respect to the surface normal, and the target recoils were detected

75 at an angle of  $45^\circ$ . The spectra was analyzed using the CONTES code for conversion to  
76 composition depth profile.<sup>16,17</sup> The Seebeck coefficient and in-plane electrical resistivity of  
77 the film were simultaneously measured from room temperature up to  $\sim 800$  K by an ULVAC-  
78 RIKO ZEM3 system in vacuum with a low-pressure helium atmosphere. The substrate  
79 contribution to the Seebeck coefficient and electrical resistivity is negligible. Hall-effect  
80 measurements were done at room temperature in van der Pauw configuration with four  
81 symmetrical electrodes and platinum contacts bonded by gold wires to the electrodes.

82

83 Figure 1(a) shows a  $\theta - 2\theta$  XRD pattern from an as-deposited ScN film. The pattern shows the  
84 ScN  $111$  diffraction peak at a  $2\theta$  angle of  $34.33^\circ$  corresponding very well to ICDD PDF 45-  
85 0978 as well as the  $\text{Al}_2\text{O}_3(0001)$  substrate peak. From the  $111$  peak position of the ScN film,  
86 the lattice parameter was determined to be  $4.51 \text{ \AA}$ . The inset of Fig. 1 shows a  $\phi$ -scan of ScN  
87  $200$  at  $40.16^\circ$ . The six peaks are due to diffraction from planes of the  $\{200\}$  family. The three-  
88 fold symmetry of the  $[200]$  orientation in a cubic crystal should give three peaks; the fact that  
89 there are six shows that there are twin-domains because of different stacking sequences in  
90 which ScN(111) can be grown on  $\text{Al}_2\text{O}_3(0001)$ . The expected epitaxial relationship for the  
91 ScN(111) grown onto the  $\text{Al}_2\text{O}_3(0001)$  surface would be  $\langle 1\bar{1}0 \rangle_{\text{ScN}} \parallel \langle 10\bar{1}0 \rangle_{\text{Al}_2\text{O}_3}$  in-plane  
92 and  $(111)_{\text{ScN}} \parallel (0001)_{\text{Al}_2\text{O}_3}$  out of plane. However, XRD shows that the  $\langle 110 \rangle$  directions of the  
93 ScN domains are here rotated in average  $\pm 4^\circ$  compare to the  $\langle 10\bar{1}0 \rangle$  direction on the  
94 sapphire surface. This effect may be due to minimize the stresses resulting from the 17%  
95 positive mismatch between the ScN and sapphire lattices and weak interaction from second or  
96 third nearest neighbor of rhombohedral/cubic stacking.

97

98 Figure 2(a) is an overview cross-section TEM image of a typical ScN film. It can be seen that  
99 the film has columnar domains and a thickness of  $\sim 180$  nm. Fig. 2(b) shows a high-resolution

100 image of the interface area of film and substrate. The image shows the epitaxial growth of  
101 ScN on Al<sub>2</sub>O<sub>3</sub>, consistent with XRD. Fig. 2(c) shows a high resolution TEM image with a  
102 lattice parameter  $a$  of ScN which agrees with that observed by XRD. ERDA showed that the  
103 film composition is 49.6±1.5 at.% of Sc and 49.3±1.5 at.% of N, i.e., close to stoichiometric.  
104 There are trace amounts of F, O, and C (~0.7 at.%, ~0.3 at.%, and ~0.1 at.%, respectively).  
105 The source of the fluorine is from the Sc target due to the production process. The appearance  
106 of the films is transparent orange, which indicates that the composition is close to  
107 stoichiometric.<sup>10,12</sup>

108  
109 The thermoelectric properties of ScN are shown in Figure 3(a) and (b). At 800 K, the Seebeck  
110 coefficient is ~-86  $\mu\text{V/K}$  and the in-plane electrical resistivity is ~2.94  $\mu\Omega\cdot\text{m}$ , giving a power  
111 factor of  $2.5\times 10^{-3} \text{ W/m}\cdot\text{K}^2$ . By assuming the literature value for the thermal conductivity of  
112 ScN,<sup>4</sup> the ZT value can be estimated to ~0.2 at 800 K. This should be considered a lower limit  
113 of ZT. Even so, it is comparable to such established thermoelectric materials as  
114 polycrystalline Ca<sub>3</sub>Co<sub>4</sub>O<sub>9</sub>.<sup>18</sup> In comparison with other transition-metal (like CrN), the ScN is  
115 five times larger in ZT value.<sup>19</sup> The measurements were performed in several cycles from  
116 room temperature to 800 K to ensure the obtained results are reproducible. Fig. 3(b) shows the  
117 repeated power factor measurement; the values are virtually identical. The diffraction pattern  
118 of the ScN was also unchanged after three cycles from room temperature to 800 K,  
119 confirming the structural stability of the ScN films in this temperature range.

120  
121 The results show that our ScN films have a relatively high (negative) Seebeck coefficient for  
122 transition-metal nitrides in combination with a high electrical conductivity, resulting in a  
123 remarkably high thermoelectric power factor. In order to tentatively explain this phenomenon,  
124 we note that the conductivity is metallic-like both in magnitude and temperature-dependence.

125 Hall measurements at room temperature yielded an electron concentration of  $1.0 \times 10^{21} \text{ cm}^{-3}$   
126 and an electron mobility of  $30.0 \text{ cm}^2 \text{ V}^{-1} \text{ s}^{-1}$ . This may be due to small contamination from  
127 oxygen, fluorine or nitrogen vacancies acting as dopants to increase carrier concentration.  
128 Additionally, the impurities might cause rapidly changing features in the density of states near  
129 the Fermi level. It has been theoretically predicted that nitrogen vacancies have this role in  
130 ScN and it is reasonable that dopants could yield a similar effect.<sup>7</sup> Preliminary calculations  
131 support this notion.<sup>20</sup> Such features in the density of states would correspond to the Mahan  
132 and Sofo prediction of the transport-distribution function that maximizes ZT.<sup>21</sup>  
133  
134 Additional samples (not shown) with higher oxygen contents (1-3 at.%) and/or  
135 substoichiometric in nitrogen, exhibited Seebeck coefficients somewhat lower, but of the  
136 same order as shown in Fig. 3(a). However, they also exhibited large difference in electrical  
137 resistivity, i.e., up to one order of magnitude higher electrical resistivity for 1-3 at.% O  
138 content than the ScN films with ~0.3 at.% O content. Hall measurements for ScN with ~1-3  
139 at.% O show an electron concentration increase to  $1.25 \times 10^{21} - 1.75 \times 10^{21} \text{ cm}^{-3}$  and electron  
140 mobilities in the range  $0.5 - 1.6 \text{ cm}^2 \text{ V}^{-1} \text{ s}^{-1}$ . This may be due to either incorporation of O in  
141 ScN or formation of secondary phases, e.g., amorphous oxides. According to the Mott  
142 equation, the Seebeck coefficient is independent of mobility if the mobility is energy-  
143 independent, therefore these data are consistent with the large reduction in conductivity (due  
144 to reduced mobility) and limited reduction in Seebeck coefficient. These observations of large  
145 variation in properties emphasize the importance of impurities and defects. The only previous  
146 report on thermoelectric properties of ScN reported a relatively modest power factor for “bulk  
147 ScN” without providing any information about the samples or their purity.<sup>22</sup>

148

149 In conclusion, the thermoelectric properties of epitaxial ScN thin films have been studied in  
150 detail. It is possible to obtain ScN exhibiting a remarkably high power factor  $2.5 \times 10^{-3}$   
151  $\text{W}/(\text{m} \cdot \text{K}^2)$  at 800 K which corresponds to a relatively high Seebeck coefficient of  $\sim -86 \mu\text{V}/\text{K}$   
152 while retaining a rather low and metallic-like electrical resistivity ( $\sim 2.94 \mu\Omega \cdot \text{m}$ ). The  
153 estimated lower limit of ZT is  $\sim 0.2$  at 800 K, which suggests that the ScN-based materials as  
154 candidates for high-temperature thermoelectrics application.

155

#### 156 ACKNOWLEDGMENT

157 Funding from the Swedish Research Council (VR, grant number 621-2009-5258) is  
158 acknowledged.

159

#### 160 REFERENCES

- 161 <sup>1</sup>G. J. Snyder and E. S. Toberer, *Nat. Mater.* **7**, 105 (2008).
- 162 <sup>2</sup>F. J. DiSalvo, *Science* **285**, 703 (1999).
- 163 <sup>3</sup>D. Gall, I. Petrov, N. Hellgren, L. Hultman, J. E. Sundgren, and J. E. Greene, *J. Appl. Phys.*  
164 **84**, 6034 (1998).
- 165 <sup>4</sup>V. Rawat, Y. K. Koh, D. G. Cahill, and T. D. Sands, *J. Appl. Phys.* **105**, 024909 (2009).
- 166 <sup>5</sup>D. Gall, M. Städele, K. Järrendahl, I. Petrov, P. Desjardins, R. T. Haasch, T.-Y. Lee, and J.  
167 E. Greene, *Phys. Rev. B* **63**, 125119 (2001).
- 168 <sup>6</sup>C. Stampfl, W. Mannstadt, R. Asahi, and A. J. Freeman, *Phys. Rev. B* **63**, 155106 (2001).
- 169 <sup>7</sup>M. G. Moreno-Armenta and G. Soto, *Computational Materials Science* **40**, 275 (2007).
- 170 <sup>8</sup>W. R. L. Lambrecht, *Phys. Rev. B* **62**, 13538 (2000).
- 171 <sup>9</sup>H. A. Al-Britthen, A. R. Smith, and D. Gall, *Phys. Rev. B* **70**, 045303 (2004).
- 172 <sup>10</sup>H. A. H. Al-Britthen, E. M. Trifan, D. C. Ingram, A. R. Smith, and D. Gall, *J. Cryst. Growth*  
173 **242**, 345 (2002).



- 174 <sup>11</sup>M. A. Moram, Z. H. Barber, and C. J. Humphreys, *Thin Solid Films* **516**, 8569 (2008).
- 175 <sup>12</sup>G. Travaglini, F. Marabelli, R. Monnier, E. Kaldis, and P. Wachter, *Phys. Rev. B* **34**, 3876  
176 (1986).
- 177 <sup>13</sup>J. M. Gregoire, S. D. Kirby, G. E. Scopelianos, F. H. Lee, and R. B. van Dover, *J. Appl.*  
178 *Phys.* **104**, 074913 (2008).
- 179 <sup>14</sup>J. P. Dismukes, W. M. Yim, J. J. Tietjen, and R. E. Novak, *R.C.A. Review* **31**, 680 (1970).
- 180 <sup>15</sup>D. H. Trinh, H. Hogberg, J. M. Andersson, M. Collin, I. Reineck, U. Helmersson, and L.  
181 Hultman, *J. Vac. Sci. Technol. A* **24**, 309 (2006).
- 182 <sup>16</sup>M. S. Janson, CONTES, Conversion of Time-Energy Spectra A Program for ERDA Data  
183 Analysis, Internal Report, Uppsala University, 2004.
- 184 <sup>17</sup>H. J. Whitlow, G. Possnert, and C. S. Petersson, *Nucl. Instrum. Meth. B* **27**, 448 (1987).
- 185 <sup>18</sup>N. V. Nong, N. Pryds, S. Linderoth, and M. Ohtaki, *Adv. Mater.* **23**, 2484 (2011).
- 186 <sup>19</sup>C. X. Quintela, F. Rivadulla, and J. Rivas, *Appl. Phys. Lett.* **94**, 152103 (2009).
- 187 <sup>20</sup>G. Soto, M. G. Moreno-Armenta, and A. Reyes-Serrato, [arXiv:0803.3644v1](https://arxiv.org/abs/0803.3644v1)[cond-mat.mtrl-  
188 sci], epublished (2008).
- 189 <sup>21</sup>G. D. Mahan and J. O. Sofo, *Proc. Nat. Acad. Sci. USA* **93**, 4436 (1996).
- 190 <sup>22</sup>M. Zebarjadi, Z. Bian, R. Singh, A. Shakouri, R. Wortman, V. Rawat, and T. Sands, *J.*  
191 *Electron. Mater.* **38**, 960 (2009).

192

193 FIGURE CAPTIONS

194 FIG 1.  $\theta$ - $2\theta$  x-ray diffraction pattern from a ScN film deposited onto an  $\text{Al}_2\text{O}_3(0001)$   
195 substrate. The inset shows a  $\phi$ -scan plot of (solid line) the ScN  $200$  plane and (dot line) the  
196  $\text{Al}_2\text{O}_3 10\bar{1}4$  plane.

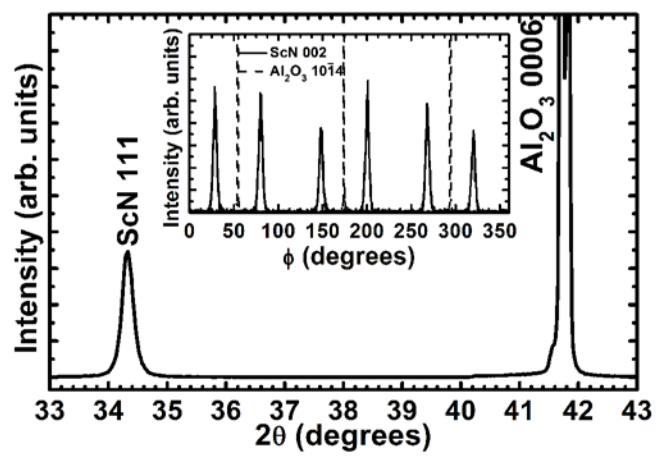
197

198 FIG 2. Cross-sectional TEM micrographs of a ScN film on  $\text{Al}_2\text{O}_3(0001)$  substrate in (a)  
199 overview and (b) high resolution of the film/substrate interface, and (c) high-resolution of a  
200 region in the bulk of the film.

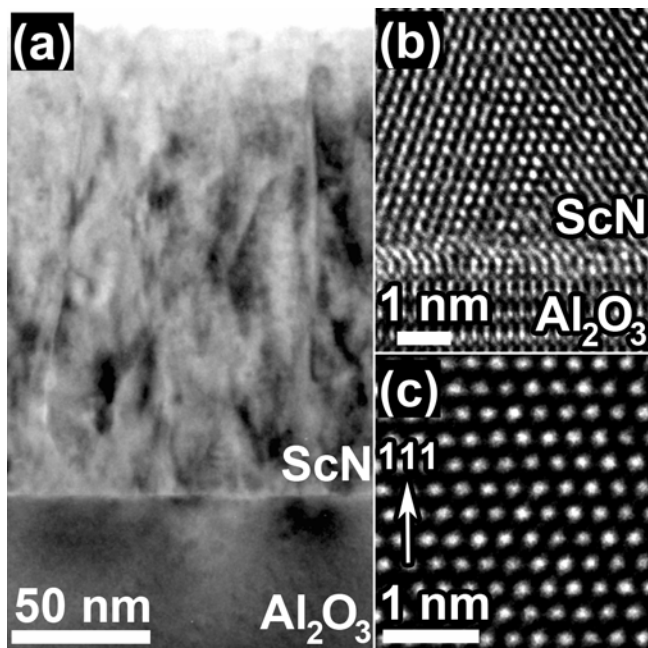
201

202 FIG 3. (color online) Thermoelectric properties of a ScN film was measured from room  
203 temperature to 800 K, (a) Seebeck coefficient (*left*) and electrical resistivity (*right*) as  
204 functions of temperature, and (b) Power factor  $S^2/\rho$  vs. temperature from 300 – 800 K for  
205 three measured cycles.

206

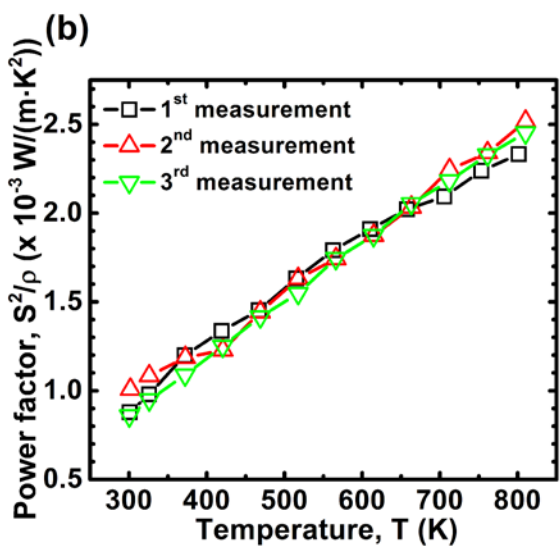
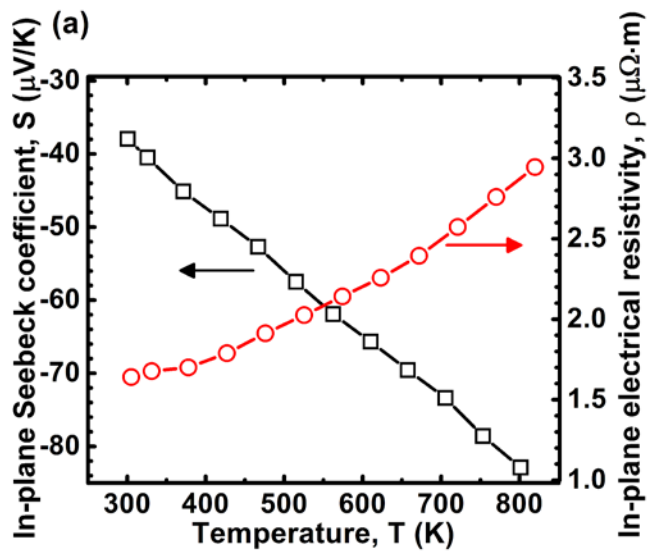


207



208

209



210